

Crystal structure analysis of two crystalline bis(ω -hydroxyalkoxy)biphenyls using a combination of powder diffraction, IR spectroscopy and molecular simulation

Arjen van Langevelde,^{a*} Pavla Capková,^{a,b} Ed Sonneveld,^a Henk Schenk,^a Miroslava Trchova^b and Michal Ilavský^{b,c}

^aLaboratory for Crystallography, Institute for Molecular Chemistry, Universiteit van Amsterdam, Nieuwe Achtergracht 166, 1018 W V Amsterdam, The Netherlands, ^bFaculty of Mathematics and Physics, Charles University, Ke Karlovu 3, 12116 Prague 2, Czech Republic, and ^cInstitute of Macromolecular Chemistry, Academy of Sciences of CzR, 16206 Prague 6, Czech Republic. E-mail: arjen@crys.chem.uva.nl

(Received 26 February 1999; accepted 8 June 1999)

Synchrotron and standard X-ray powder diffraction (XRD) combined with IR spectroscopy and molecular simulations have been used to investigate the crystal structure of two crystalline mesogenic diols: 4,4'-bis(6-hydroxy-1-hexyloxy)biphenyl (D-I) and 4,4'-bis(11-hydroxy-1-undecyloxy)biphenyl (D-II). The crystal structure of D-I has been determined from high-resolution synchrotron powder-diffraction data collected at BM16 of the ESRF. The methods of grid search and Rietveld refinement have been used to determine this structure. The space group is *Cc*, with unit-cell parameters $a = 44.392(3)$, $b = 7.221(1)$, $c = 6.631(1)$ Å and $\beta = 91.09(1)^\circ$. The structure of D-II has a small degree of disorder. This structure was analyzed with a combination of experimental methods, conventional XRD, IR spectroscopy and molecular mechanics simulations, revealing the character of the structural disorder. Both the structures of D-I and D-II are lamellar-packed and layered. The hydrogen-bonding system between two adjacent layers in the structure of D-II is distorted.

Keywords: liquid crystal; molecular simulation; powder diffraction; structure determination.

1. Introduction

Polyurethane systems based on diols and diisocyanates with amorphous, semi-crystalline or liquid-crystalline structure have been widely studied in the literature (Ilavský *et al.*, 1998). These systems are mainly applied in fibres, elastomers, foams and coatings. Modification of the monomer units directly affects the structure and properties of these polymers. Introduction of a stiff anisotropic mesogenic group to either the diol or diisocyanate lead to polyurethanes with thermotropic liquid-crystal properties (Penczek *et al.*, 1993; Stenhouse *et al.*, 1989; Tanaka & Nakaya, 1989). These mesogenic groups in the polyurethane tend to form crystalline phases with very high phase-transition temperatures and melting points. To decrease the phase-transition temperature a flexible chain is added to the rigid aromatic skeleton.

The present structure analysis of crystalline diols with a mesogenic group and a flexible hydrocarbon chain represents the first step in structural studies of polyurethane systems, based on this type of diol. In the present paper the structure determination and analysis of two crystalline bis(ω -hydroxyalkoxy)biphenyl compounds are described. For brevity the diols 4,4'-bis(6-hydroxy-1-hexyloxy)biphenyl and 4,4'-bis(11-hydroxy-1-undecyloxy)biphenyl are

hereon denoted as D-I and D-II. Fig. 1 shows the chemical structure diagram of these molecules. Both diols are available in crystalline powder form only. Therefore, the methods of grid search and Rietveld refinement have been used to determine the ordered crystal structure of D-I from high-resolution synchrotron powder-diffraction data. The crystal structure of D-II exhibits a certain degree of disorder; X-ray powder diffraction and IR spectroscopy were therefore combined with molecular mechanics simulations to obtain the main structural features, responsible

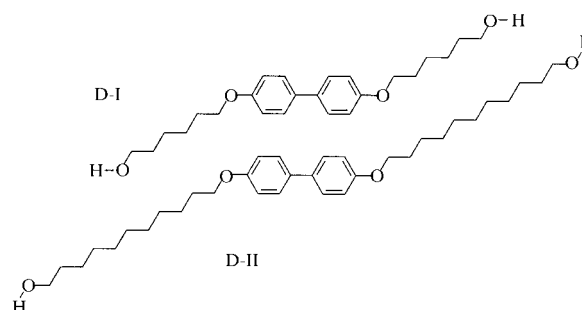


Figure 1 Schematic chemical structure diagram of 4,4'-bis(6-hydroxy-1-hexyloxy)biphenyl (D-I) and 4,4'-bis(11-hydroxy-1-undecyloxy)biphenyl (D-II).

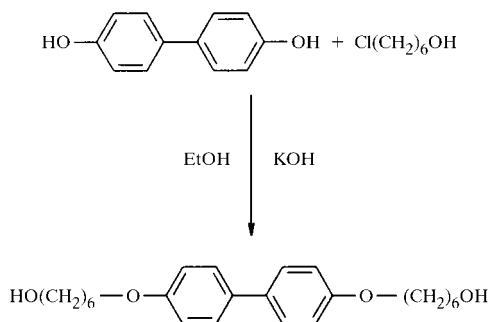
for partial long-range ordering, and to characterize the disorder in the D-II crystal structure.

2. Experimental and modelling strategy

2.1. Synthesis of diols D-I and D-II

Mesogenic diols D-I and D-II were prepared at the Institute of Macromolecular Chemistry, Czech Academy of Sciences.

Synthesis of D-I was carried out as follows (see scheme). 4,4'-Bis(6-hydroxy)biphenyl (0.03 mol) was added to a



solution of KOH (0.06 mol) in 200 ml of ethanol. After addition of 6-chloro-1-hexanol (0.09 mol) the mixture was stirred for 72 h at 363 K. The product was filtered off and the residue was recrystallized from benzene/ethanol mixture (1/2 by volume). After three recrystallizations a white solid product with an observed melting point of 448–449 K was obtained. Elemental analysis for $C_{24}H_{34}O_4$ showed found/calculated values of 74.68/74.57 wt% C and 8.95/8.86 wt% H.

Synthesis of D-II was carried out by a similar procedure. In this case, 11-bromo-1-undecanol was used instead of 6-chloro-1-hexanol. The crystallization was carried out from toluene/ethanol mixture (1/2 by volume); the observed melting point of the product was 428–429 K. Elemental analysis for $C_{34}H_{54}O_4$ showed found/calculated values of 77.40/77.51 wt% C and 10.17/10.32 wt% H.

2.2. Synchrotron and X-ray powder diffraction

X-ray powder-diffraction photographs of these samples were taken using an Enraf-Nonius FR 552 Guinier Johansson camera (Enraf-Nonius, Delft, The Netherlands) equipped with a Johansson monochromator (Roberts & Parrish, 1962) using $Cu K\alpha_1$ radiation ($\lambda = 1.54060 \text{ \AA}$). The samples were prepared by pressing the powder into a thin layer onto Mylar foil. To improve particle statistics the sample holder was rotated in the specimen plane. For indexing of the patterns the accurate positions of as many lines as possible were collected by reading out the Guinier photographs with an optical instrument. Using a Johansson LS-18 microdensitometer the Guinier photographs were digitized from 4.0 to $84.2^\circ 2\theta$ in steps of $0.01^\circ 2\theta$.

An X-ray powder-diffraction pattern of D-I was measured at the high-resolution powder diffractometer (BM16; Fitch, 1996) at the European Synchrotron Radi-

ation Facility (ESRF, Grenoble, France) with $\lambda = 0.4093008 \text{ \AA}$. This wavelength was calibrated by measuring 11 peaks from *NIST* Si standard 640b (lattice parameter certified as 5.43094 \AA). These peaks were fitted with a pseudo-Voigt profile function to obtain peak positions, accounting for asymmetry using the Finger–Cox–Jephcoat correction, and then fitting the wavelength and instrumental zero point to these positions *via* least-squares methods. For data collection a capillary with a diameter of 1.5 mm was filled with powder and rotated during exposure. Continuous scans were made from 0.0 to $25.0^\circ 2\theta$ with $0.5^\circ 2\theta \text{ min}^{-1}$ and a sampling time of 50 ms . After data collection the scans were binned at $0.005^\circ 2\theta$.

In order to obtain well defined texture, an additional standard powder-diffraction pattern in Bragg–Brentano geometry (flat samples) has been made for D-II using an HZG4 diffractometer (Fig. 8). The measured pattern with well defined texture (*i.e.* cylindro-symmetrical, with the texture axis perpendicular to the flat sample surface) was necessary for comparison with the calculated diffraction patterns (see §2.4).

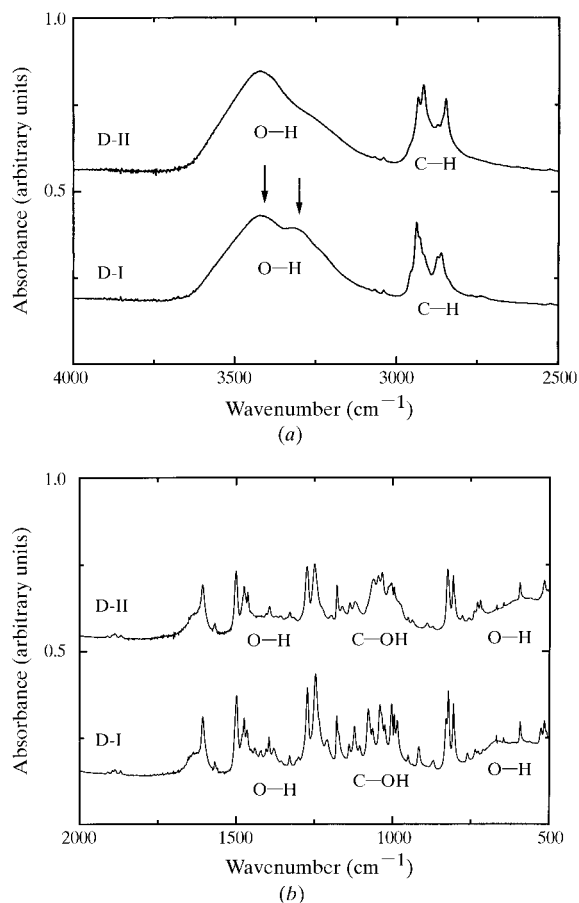


Figure 2

Comparison of the IR absorption spectra of D-I and D-II (a) in the region 4000 – 2500 cm^{-1} , and (b) in the region 2000 – 500 cm^{-1} . Peaks corresponding to the two distinct O–H stretching bands in the dimeric hydrogen-bonding system are marked by arrows.

2.3. Infrared spectroscopy

Vibrational properties of the samples were measured using Fourier transform infrared (FTIR) spectroscopy. The measurements were performed on a Nicolet IMPACT 400 FTIR spectrometer in an H₂O-purged environment. All spectra in the range 400–4000 cm⁻¹ with 2 cm⁻¹ spectral resolution were obtained from compressed KBr pellets in which either the D-I or the D-II powder sample was evenly dispersed. 200 scans were summed to obtain the FTIR spectrum.

The IR absorption spectra for both D-I and D-II exhibit the same positions of absorption bands, characteristic for these kind of compounds (Holly & Sohar, 1975; Silverstein *et al.*, 1991): the aromatic C–H stretching (weak bands between 3100 and 3000 cm⁻¹); asymmetrical and symmetrical stretching $\nu_{as}(\text{CH}_2)$ and $\nu_s(\text{CH}_2)$ occurring near 2926 and 2853 cm⁻¹, respectively; the scissoring band $\delta_s(\text{CH}_2)$ between 1500 and 1450 cm⁻¹; the split C–O–C asymmetrical stretching band between 1300 and 1200 cm⁻¹ and the out-of-plane C–H bending of ring H atoms between 850 and 700 cm⁻¹. Besides these common features, the IR spectra of D-I and D-II show pronounced differences (Fig. 2). All these differences occur in the frequency regions corresponding to the following O–H vibrations:

(i) O–H stretching mode $\nu(\text{OH})$ between 3650 and 3200 cm⁻¹;

(ii) O–H in-plane bending $\beta(\text{OH})$ coupled with C–H wagging vibration producing two bands between 1420 and 1330 cm⁻¹;

(iii) C–O(H) stretching band $\nu(\text{C–OH})$, which usually appears between 1230 and 1000 cm⁻¹;

(iv) O–H out-of-plane deformation vibration $\delta(\text{OH})$, which is of little diagnostic value, as the interval of appearance is very wide (1000–200 cm⁻¹), and the band is very broad, because it is composed of several sub-maxima.

The consequences of the different O–H vibrations in D-I and D-II will be discussed in detail in §4.

2.4. Strategy of modelling

Molecular mechanics simulations, based on the *pcff_300* force field, have been used to optimize the conformation and crystal packing of the diols. The modelling was performed with the program *Cerius²* (Molecular Simulations Inc., 1995). For a description of *Cerius²* see, for example, Comba & Hambley (1995). The *pcff_300* force field (Sun *et al.*, 1994) was developed for application to polymers and organic materials. The molecular crystal structure of 4-(6-hydroxy-1-hexyloxy)-4'-hydroxybiphenyl, as taken from the Cambridge Structural Database (Allen & Kennard, 1993) with reference code WEBWAB, was used to test the suitability of the various force fields available in *Cerius²*: *pcff_300*, *cvff_300* and *cvff_950* (Hagler *et al.*, 1974). The mutual positions of molecules in the calculated and experimental models showed the same characteristics for all the tested force fields. However, the calculated cell parameters *a* and *b* differ from the experimental values by

Table 1

Fractional atomic coordinates and thermal parameters (U_{iso}) for D-I after the bond-restrained Rietveld refinement.

Cell parameters of D-I: $a = 44.392(3)$, $b = 7.221(1)$, $c = 6.631(1)$ Å and $\beta = 91.09(1)^\circ$. The volume is 2125.2(5) Å³ and the space group is *Cc*, with $Z = 4$ resulting in a density of 1.21 g cm⁻³.

| Atom | <i>x</i> | <i>y</i> | <i>z</i> | U_{iso} (Å ²) |
|------|----------|----------|----------|------------------------------------|
| O1 | 0.0862 | 0.3030 | 0.6311 | 8.3793 |
| O2 | -0.0779 | 0.2571 | 1.2704 | 8.3793 |
| O3 | 0.2244 | 0.1794 | -0.5136 | 8.3793 |
| O4 | 0.3751 | 0.3321 | -1.2779 | 8.3793 |
| C5 | 0.1582 | 0.1692 | -0.1860 | 8.3347 |
| C6 | 0.1471 | 0.2589 | 0.1586 | 8.3347 |
| C7 | 0.1361 | 0.3563 | 0.4968 | 8.3347 |
| C8 | 0.1194 | 0.1634 | 0.1602 | 8.3347 |
| C9 | 0.1072 | 0.2827 | 0.4803 | 8.3347 |
| C10 | 0.0977 | 0.2109 | 0.3003 | 8.3347 |
| C11 | 0.0524 | 0.2612 | 0.5883 | 8.3347 |
| C12 | 0.0398 | 0.2887 | 0.8032 | 8.3347 |
| C13 | 0.0078 | 0.2639 | 0.8146 | 8.3347 |
| C14 | -0.0050 | 0.2492 | 1.0296 | 8.3347 |
| C15 | -0.0385 | 0.2244 | 1.0295 | 8.3347 |
| C16 | -0.0468 | 0.2538 | 1.2819 | 8.3347 |
| C17 | 0.1545 | 0.3608 | 0.3281 | 8.3347 |
| C18 | 0.1682 | 0.2344 | 0.0051 | 8.3347 |
| C19 | 0.1808 | 0.1239 | -0.3272 | 8.3347 |
| C20 | 0.1959 | 0.3369 | 0.0164 | 8.3347 |
| C21 | 0.2096 | 0.2047 | -0.3080 | 8.3347 |
| C22 | 0.2178 | 0.2988 | -0.1312 | 8.3347 |
| C23 | 0.2563 | 0.2390 | -0.5046 | 8.3347 |
| C24 | 0.2662 | 0.2245 | -0.7208 | 8.3347 |
| C25 | 0.2991 | 0.2554 | -0.7400 | 8.3347 |
| C26 | 0.3083 | 0.2529 | -0.9652 | 8.3347 |
| C27 | 0.3407 | 0.2754 | -0.9951 | 8.3347 |
| C28 | 0.3460 | 0.3137 | -1.2462 | 8.3347 |
| H29 | 0.1357 | 0.1665 | -0.2205 | 5.0000 |
| H30 | 0.1121 | 0.1183 | 0.0233 | 5.0000 |
| H31 | 0.0782 | 0.1528 | 0.2817 | 5.0000 |
| H32 | 0.0539 | 0.1985 | 0.9202 | 5.0000 |
| H33 | 0.0510 | 0.1196 | 0.5526 | 5.0000 |
| H34 | 0.0453 | 0.4360 | 0.8466 | 5.0000 |
| H35 | 0.0432 | 0.3489 | 0.4900 | 5.0000 |
| H36 | 0.0077 | 0.1422 | 1.1181 | 5.0000 |
| H37 | 0.0017 | 0.1208 | 0.7552 | 5.0000 |
| H38 | 0.0038 | 0.3939 | 1.1038 | 5.0000 |
| H39 | -0.0035 | 0.3642 | 0.7126 | 5.0000 |
| H40 | -0.0366 | 0.1469 | 1.3664 | 5.0000 |
| H41 | -0.0443 | 0.1036 | 0.9757 | 5.0000 |
| H42 | -0.0400 | 0.3901 | 1.3525 | 5.0000 |
| H43 | -0.0490 | 0.3475 | 0.9584 | 5.0000 |
| H44 | -0.0894 | 0.3117 | 1.1824 | 5.0000 |
| H45 | 0.1385 | 0.4569 | 0.5991 | 5.0000 |
| H46 | 0.1774 | 0.0220 | -0.4368 | 5.0000 |
| H47 | 0.1704 | 0.4554 | 0.3149 | 5.0000 |
| H48 | 0.2031 | 0.3774 | 0.1606 | 5.0000 |
| H49 | 0.2535 | 0.2927 | -0.8023 | 5.0000 |
| H50 | 0.2384 | 0.3623 | -0.1195 | 5.0000 |
| H51 | 0.2585 | 0.3596 | -0.4641 | 5.0000 |
| H52 | 0.2637 | 0.0888 | -0.7532 | 5.0000 |
| H53 | 0.2674 | 0.1634 | -0.4163 | 5.0000 |
| H54 | 0.2963 | 0.3522 | -1.0322 | 5.0000 |
| H55 | 0.3042 | 0.3769 | -0.6919 | 5.0000 |
| H56 | 0.3018 | 0.1343 | -1.0221 | 5.0000 |
| H57 | 0.3108 | 0.1719 | -0.6695 | 5.0000 |
| H58 | 0.3357 | 0.4117 | -1.2832 | 5.0000 |
| H59 | 0.3450 | 0.4098 | -0.9554 | 5.0000 |
| H60 | 0.3389 | 0.2003 | -1.3066 | 5.0000 |
| H61 | 0.3514 | 0.1981 | -0.9494 | 5.0000 |
| H62 | 0.3711 | 0.3443 | -1.4390 | 5.0000 |

about 10% for all force fields, attributing to the biphenyl being in the centre of the chains. The best results, as to the

conformation of the molecules, have been obtained with the force field *pcff_300*, which was chosen for modelling of D-I and D-II structures.

For several crystal structure models X-ray powder-diffraction patterns were calculated. To compare these calculated patterns with the measured textured patterns, a texture correction procedure is used. The only type of texture correction available in *Cerius*² is cylindro-symmetrical, according to March–Dollase (Dollase, 1986).

3. Structure determination of D-I

3.1. Structure solution and refinement of D-I

The synchrotron diffraction pattern of D-I was indexed using the program *ITO* (Visser, 1969). The resulting cell parameters were refined to $a = 44.392(3)$, $b = 7.221(1)$, $c = 6.631(1)$ Å and $\beta = 91.09(1)^\circ$ using the program *UnitCell* (Holland & Redfern, 1997). The pattern shows reflection conditions $hkl: h + k = 2n$ and $h0l: l = 2n$, corresponding to a *C*-face-centred monoclinic cell and a *c*-glide implying one of the space groups *Cc* or *C2/c*. The cell has a volume of $2125.2(5)$ Å³ and with four molecules in the unit cell the calculated density is 1.21 g cm⁻³. The calculation was performed, for space group *Cc*, with one molecule per asymmetric unit and, for space group *C2/c*, with a half molecule per asymmetric unit. To obtain accurate reflection intensities a full-pattern decomposition (FPD) procedure was started. The synchrotron powder-diffraction pattern was fitted with a mathematical function ($R_p = 9.08\%$, $R_{wp} = 12.75\%$ and $\chi^2 = 4.67$) and decomposed using the program *MRIA* (Zlokazov & Chernyshev, 1992).

A starting structure model for D-I has been made using the program *Cerius*² (Molecular Simulations Inc., 1995), originating from the molecular structure of 4-(6-hydroxy-1-hexyloxy)-4'-hydroxybiphenyl, reference code WEBWAB (Allen & Kennard, 1993). The H atom of the 4'-hydroxyphenyl of WEBWAB was replaced by hexanol resulting in a possible molecular model of D-I. The energy of this model was minimized, keeping the 4-(6-hydroxy-1-hexyloxy)-4'-hydroxybiphenyl part constrained.

To locate this possible model in the asymmetric unit of the cell with space group *Cc*, a grid search procedure (Chernyshev & Schenk, 1998) was applied using the reflection intensities obtained from the full-pattern decomposition procedure. The obtained translational and rotational parameters were refined followed by a bond-restrained Rietveld refinement. The biphenyl rings were kept fixed, while the coordinates of the remainder atoms as well as the thermal parameters (U_{iso}) for the C and O atoms were refined, resulting in a final structure with $R_p = 10.54\%$, $R_{wp} = 2.83\%$ and $\chi^2 = 5.66$ (Table 1, Fig. 3). This is reasonably good for long-chain organic molecules. Nevertheless, small misfits can be observed in the region between 10 and $15^\circ 2\theta$ (Fig. 3). The few high-intensity reflections (d -value range 3.5 – 5.0 Å), originating from the lateral packing of the hydrocarbon chains, dominate the structure refinement, in a similar way as found in triacylglycerols (Van Langevelde *et al.*, 1999). Atoms between these chains, like the biphenyls in these diols and glycerol in triacylglycerols, contribute only small intensities. Consequently, these groups of atoms could not be refined properly and were restrained during structure refinement.

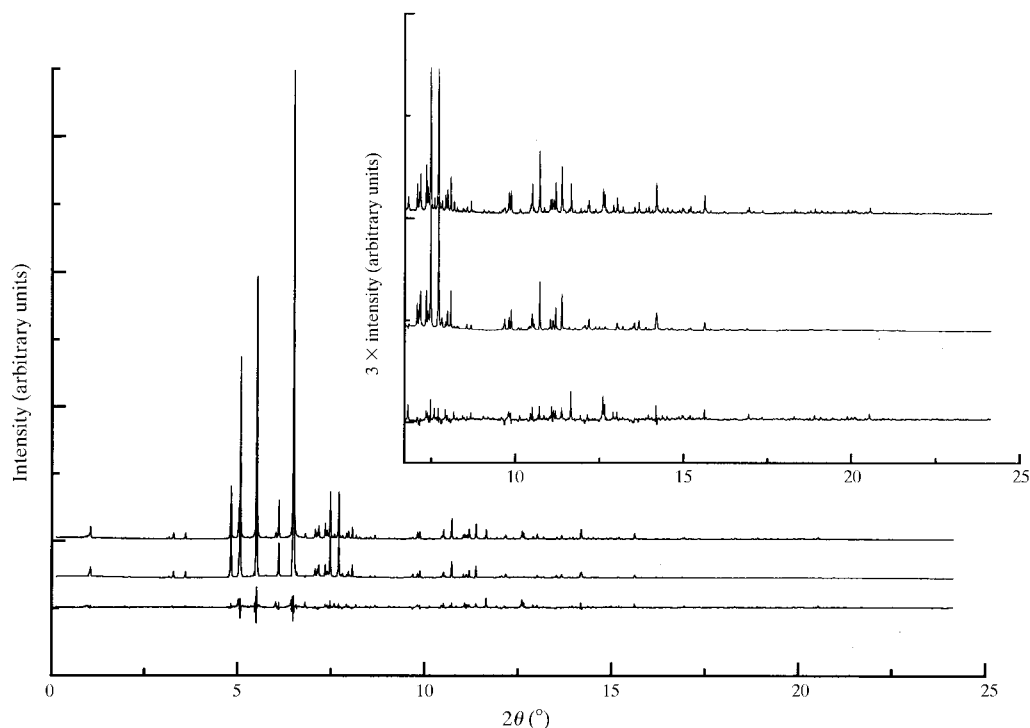


Figure 3

Synchrotron powder-diffraction pattern ($\lambda = 0.4093008$ Å) of D-I (upper), the pattern as calculated from the refined crystal structure (middle) and the difference between these patterns (lower). The inset shows the low-intensity reflections at high angle (6.7 – $25.0^\circ 2\theta$).

The crystal structure of D-I, as refined in space group Cc , was also tested for having $C2/c$ space group symmetry with the option *ADDSYM*, incorporated in the program *Platon98* (Spek, 1990). The agreement with this symmetry is 89%, with the outer two atoms having the largest misfit. Nevertheless, refinement of D-I in this space group was not successful. Having half a molecule in the asymmetric unit, there is no possibility to restrain the distance between the two phenyl rings. Since the refinement is dominated by the high-intensity reflections corresponding to lattice planes parallel to the hydrocarbon chain axis of the diol, the molecule can easily shift along this axis during refinement. This shift has almost no effect on the R value. Consequently, the two parts of the molecule are too close to each other resulting in an unreasonable crystal structure. However, space group $C2/c$ cannot be excluded.

Figs. 4 and 5 show the bilayer arrangement of D-I in space group Cc projected on the ac plane and the ab plane, respectively. The structure is lamellar-packed (Fig. 5) such that the diols are arranged in planes parallel to the ac plane. Two neighbouring lamellae differ in their orientation of biphenyl rings and in the orientation of O—H groups. Fig. 4 shows the structure within one lamella and Fig. 5 illustrates how the lamellae are packed in the crystal (lamellar planes are perpendicular to the ab and bc planes). The upper view of the lamellar structure is shown in Fig. 6 (projection on the bc plane, lamellar planes perpendicular to the ab planes).

The diol layers are linked *via* a system of hydrogen bonds (Fig. 7). In the case of D-I there is a regular system of hydrogen bonds between the lower and upper diols belonging to one lamella. There are no hydrogen bonds between diols in neighbouring lamellae within the limit value of the H-acceptor distance, 3 Å, which means only intralamellar hydrogen bonding occurs in D-I. Each O—H group is involved in one hydrogen bond either as donor or as acceptor. These dimeric hydrogen bonds give rise to two IR absorption bands: the first one in the range 3620–3570 cm^{-1} and the second one in the range 3590–3400 cm^{-1} (Holly & Sohar, 1975). These two distinct bands, typical for the dimeric hydrogen bonds, are present in the IR absorption spectrum of D-I (Fig. 2a).

To confirm the suitability of the chosen force field, the energy of the crystal structure of D-I as derived from the synchrotron powder-diffraction pattern was minimized using the program *Cerius²*. During this energy minimization with the *pcff_300* force field the biphenyl position as well as the cell parameters were fixed. From the resulting model the powder-diffraction pattern was calculated and fitted with the synchrotron powder-diffraction pattern ($R_p = 15.87\%$). This model structure of D-I, which corresponds to the local energy minimum as found by molecular modelling, slightly deviates from the crystal structure as derived from the synchrotron data ($R_p = 15.87\%$ versus $R_p = 10.54\%$, respectively). Most probably this was caused by shortcomings of the force field in the description of the

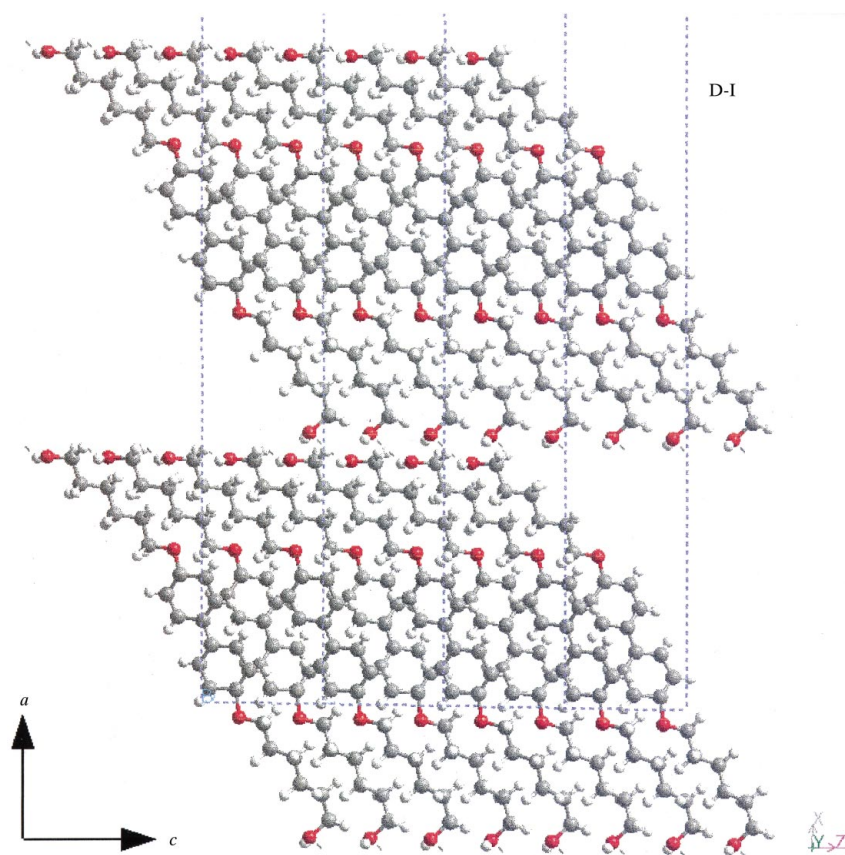


Figure 4

Structure of D-I in projection on the ac plane. The dashed line represents the unit cell. O atoms are red, C atoms are grey and H atoms are white.

energy profile for this molecule. One should be aware of these shortcomings in further considerations.

4. Structure analysis of D-II

The diffraction pattern of D-II (Fig. 8) has low resolution with broad reflections. Although there is still a high degree of long-range order, no unit cell and no space group could be established. Therefore, crystal structure determination of D-II was not possible from our powder-diffraction data.

The main task in the structure analysis of D-II was to describe the long-range ordering of the molecules and to characterize the disorder of the structure. For this purpose the conventional X-ray powder-diffraction analysis was combined with IR spectroscopy and force-field-based molecular modelling.

Comparison of the D-I and D-II IR absorption spectra showed pronounced differences in the regions corresponding to O—H vibrations and to the C—O(H) stretching band (Fig. 2). Therefore, we may conclude that the structure of D-II exhibits orientational disorder at the $(\text{CH}_2)_{11}$ chain ends, affecting especially the OH groups, accompanied with disorder of the interlayer hydrogen-bonding system. The most striking difference between the IR absorption spectra of D-II and D-I can be observed at the $3650\text{--}3200\text{ cm}^{-1}$ region, corresponding to the $\nu(\text{OH})$ stretching mode (Fig. 2a). Instead of two distinct absorption bands corresponding to a regular dimeric arrangement of hydrogen bonds as in D-I, only one smoothed band is

observed in the IR absorption spectrum of D-II. This is clear evidence that the ordered dimeric system of hydrogen bonds is broken, causing an orientational disorder of O—H groups and disorder in torsion angles at the end of the chains and resulting in disorder in layer stacking.

To elucidate the disorder and the main structural features of D-II, molecular mechanics simulations of D-II structure were performed using the *pcff_300* force field. The initial model was derived from the structure of D-I by extending the hydrocarbon chains and enlarging the *a*-axis of the unit cell to 68 Å. This value has been derived from three single non-overlapping reflections, (200), (400) and (600). The error estimated was 1 Å. Energy minimization in space group $P\bar{1}$ with variable cell parameters was carried out. During minimization the calculated X-ray powder-diffraction pattern and the difference with the experimental pattern was monitored. A series of models has been obtained with almost the same crystal energy per unit cell, but with different orientations of the O—H groups, different distortion of chain ends and, consequently, with different arrangements of hydrogen bonding. The calculated diffraction pattern of all these models fit the experimental diffraction pattern with almost the same agreement factor. Fig. 8 shows the experimental diffractogram and calculated patterns of two models of D-II structure from this series. Both models, for which the diffractograms are presented, exhibit almost the same total sublimation energy, 363.5 and $362.7\text{ kcal mol}^{-1}(\text{unit cell})^{-1}$, and their lattice parameters differ within the estimated limits (see

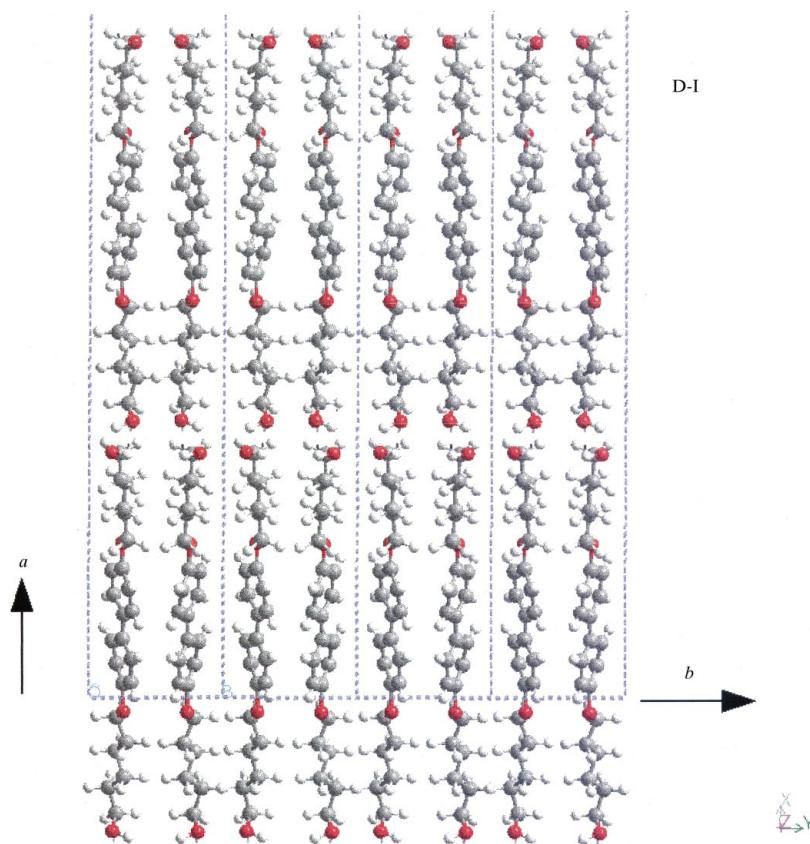
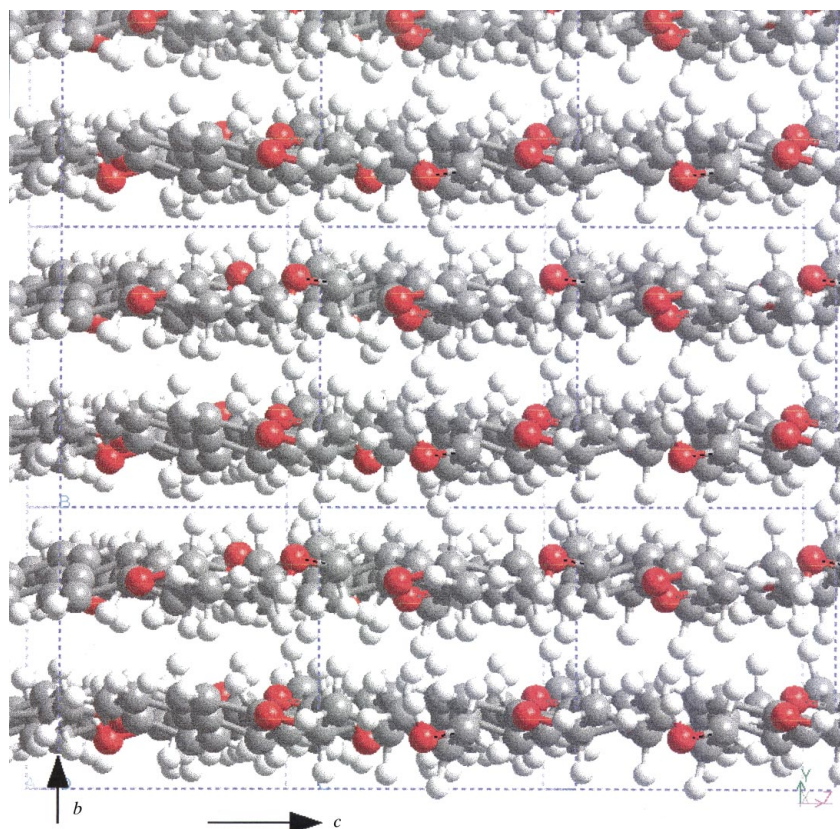


Figure 5

Structure of D-I in projection on the *ab* plane, illustrating the lamellar structure. The dashed line represents the unit cell. O atoms are red, C atoms are grey and H atoms are white.

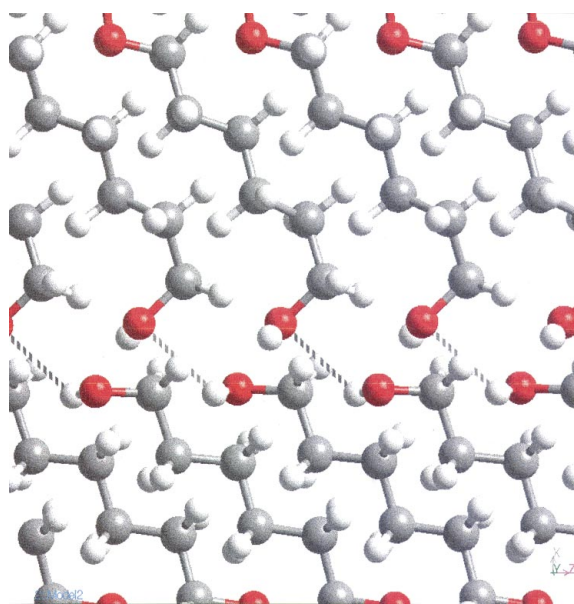
**Figure 6**

Structure of D-I in projection on the bc plane. The interlamellar distance is 3.61 Å. The dashed line represents the unit cell. O atoms are red, C atoms are grey and H atoms are white.

below). However, both models significantly differ in their chain torsions. A comparison of individual models with the experimental data is difficult as the models are three-dimensional periodical in contradiction to the experimental pattern which is the summation of all diffractograms for all models with the same crystal energy. In fact, the series of models with the same energy and with different C—C—O—H torsions in the end of chains and with slightly different cell parameters is clear evidence for the structural disorder. That means instead of one deep global minimum the system exhibits multiple minima, which are very shallow with almost the same energy. This situation is typical for disordered structures. Comparing the experimental and calculated diffraction pattern, one has to keep in mind that in the case of disordered structures the experimental pattern represents the superposition of patterns from all the strictly periodical calculated models.

This disorder manifests itself in different values of C—C—O—H torsion angles in different calculated models, exhibiting a large range of values from 50 to 170°. While for the structure of D-I the length of both hydrogen bonds in one unit cell is the same (H-acceptor distance 2.41 Å), for the structure of D-II the H-acceptor distance for intralamellar hydrogen bonding is 2.32–2.65 Å. For the structure of D-II, weak interlamellar hydrogen bonds along the b -axis were also observed (H-acceptor distance between 2.62 and 2.99 Å). This is in contrast with the structure of D-I where no interlamellar hydrogen bonds along the b -axis have been observed within the limits of the H-acceptor

distance, 3 Å. The lattice parameters of all calculated models have been obtained within the following ranges: $a = 67.7\text{--}68.9$, $b = 7.40\text{--}7.43$, $c = 6.36\text{--}6.60$ Å; $\alpha = 89.96\text{--}90.02^\circ$; $\beta = 83.56\text{--}91.1^\circ$; $\gamma = 89.91\text{--}90.13^\circ$.

**Figure 7**

Fragment of the D-I structure showing the interlayer and intralamellar hydrogen-bonding system (projection on the ac plane). Hydrogen bonds are marked with hashed lines. O atoms are red, C atoms are grey and H atoms are white.

The diol layer thickness, d_o , varied within the interval 31.52–34.34 Å together with the tilting angle of the chain axis varying between 51.3 and 54.1°. The largest scatter of values was observed for a , c and β , and almost no scatter was observed for the b , α and γ values. The large intervals for a , c and β values indicate that the structural disorder affects mostly the intralamellar structure, *i.e.* the tilting angle of the diols axis and their mutual packing within one lamella and, consequently, the layer thickness d_o . On the other hand, the b parameter, characterizing the interlamellar distance, remains almost constant in all calculated models. The α and γ parameters are close to 90° indicating that the structure maintains monoclinic (pseudo)symmetry.

The Cc space-group symmetry of the D-I structure relates the diols in the upper and lower layers in the unit cell with an axial glide plane. Therefore, the lower and upper pair of diols exhibit opposite mutual orientation (Fig. 5). However, in the case of the D-II structure where this symmetry is not present, the two layers in the unit cell still keep this orientation of diols. In fact, two different series of initial models have been built for D-II: one with the orientation of the biphenyl rings in the lower and upper layer as in D-I (Fig. 5) and one with the same orientation of biphenyl rings in the lower and upper layer. The second model is derived from the first by shifting the layers $1/2(b+c)$ in the bc plane. Both series of energy-minimized models have the same crystal energy per unit cell and probably

both are present in D-II crystals, as is evident from the line broadening in the D-II diffractogram (Fig. 8). The line broadening in the case of D-II exceeds the pure instrumental broadening, as is evident from comparison with the pattern of the standard sample (silver behenite). However, the line broadening alone is, of course, no evidence for the suggested type of disorder. The second significant evidence is the conformational behaviour of the diol D-II, which manifests itself with flexibility in the variations of C—C—O—H torsion angles, found by molecular modelling. The series of models with almost the same crystal energy and lattice parameters, but with different torsion angles in the chains, shows that the system exhibits multiple shallow energy minima resulting in disorder in the chain packing. This disorder leads to disorder in the interlayer hydrogen-bonding system (as is evident from the IR spectrum) and, consequently, to disorder in layer stacking.

5. Conclusions

The present results shows that the combination of X-ray diffraction, IR absorption spectroscopy and molecular simulations is useful in the structure analysis of partially disordered structures.

The crystal structure of a long-chain organic molecule (D-I) has been determined from high-resolution synchrotron diffraction data. Since the unit cell of this type of compound has a long and a short axis and, consequently, a huge volume, synchrotron data is absolutely necessary to obtain detailed structural information, including accurate cell parameters and intensities.

The present structure analysis of the two crystalline bis(ω -hydroxyalkoxy)biphenyls shows that the extension of alkane chains from six to 11 C atoms leads to disorder in molecular crystal packing. This disorder in 4,4'-bis(11-hydroxy-1-undecyloxy)biphenyl (D-II) manifests itself by the distortion of chain ends (large range of C—C—O—H torsion angles), as is evident from the molecular modelling results, and leads to the break up of the regular system of hydrogen bonding in the ordered structure of 4,4'-bis(6-hydroxy-1-hexyloxy)biphenyl (D-I), which was observed in the IR absorption spectrum. The main structural features, like mutual orientations of biphenyl rings of two neighbouring diols in one layer, remain the same in both structures.

This work was supported by the Grant Agency of the Charles University, Grant No. 46/1998/B and Grant No. 37/1997/B and Grant Agency of the Academy of Sciences of the Czech republic No. A4112901. One of the authors (AvL) is supported by the Netherlands Foundation for Chemical Research (NWO/CW) with financial aid from the Netherlands Technology Foundation (STW). The authors thank Dr K. Bouchal from the Institute of Macromolecular Chemistry for preparation of the diols. They thank the ESRF (Grenoble, France) for the opportunity to perform

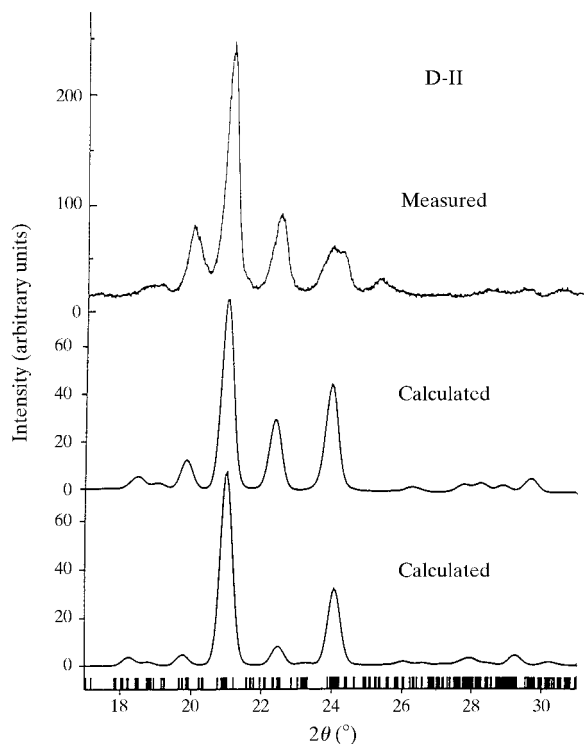


Figure 8

Experimental X-ray powder-diffraction pattern of D-II (upper) and two diffraction patterns calculated from the series of D-II models, obtained by molecular mechanics simulations (see text). Vertical bars on the 2θ scale denote the position of hkl reflections.

the synchrotron powder-diffraction experiments and to Drs A. Fitch and E. Doryhee for their invaluable help at beamline BM16.

References

- Allen, F. H. & Kennard, O. (1993). *Chem. Des. Autom. News*, **8**, 31–37.
- Chernyshev, V. V. & Schenk, H. (1998). *Z. Kristallogr.* **213**, 1–3.
- Comba, P. & Hambley, T. W. (1995). *Molecular Modeling*. Weinheim, New York: VCH.
- Dollase, W. A. (1986). *J. Appl. Cryst.* **19**, 267–272.
- Fitch, A. N. (1996). *Materials Science Forum*, Vol. 228, edited by R. J. Cernik, R. Delhez & E. J. Mittemeijer, pp. 219–222. Aedermannsdorf: Trans Tech Publications.
- Hagler, A. T., Huler, E. & Lifson, S. (1974). *J. Am. Chem. Soc.* **96**, 5319–5327.
- Holland, T. J. B. & Redfern, S. A. T. (1997). *Mineral. Mag.* **61**, 65–77.
- Holly, S. & Sohar, P. (1975). *Absorption Spectra in the Infrared Region (Theoretical and Technical Introduction)*, edited by L. Lang & W. H. Prichord, pp. 68–79. Budapest: Akademiai Kiado.
- Ilavský, M., Bouchal, K., Valentová, H., Lednický, F., Sikora, A. & Baldrian, J. (1998). *J. Macromol. Sci. Phys.* **B37**(5), 645–666.
- Langevelde, A. van, van Malssen, K., Hollander, F., Peschar, R. & Schenk, H. (1999). *Acta Cryst.* **B55**, 114–122.
- Molecular Simulations, Inc. (1995). *Cerius²*. Release 2.0. BIOSYM/Molecular Simulations Inc., San Diego, USA.
- Penczek, P., Frisch, K. C., Szczepaniak, B. & Rudnik, E. (1993). *J. Polym. Sci. Polym. Chem. Ed.* **31**, 1211–1220.
- Roberts, B. W. & Parrish, W. (1962). *International Tables for Crystallography*, Vol. III, edited by C. H. MacGillavry & G. D. Rieck, pp. 73–88. Birmingham: Kynoch Press.
- Silverstein, R. M., Bassler, C. G. & Morrill, T. C. (1991). *Spectrometric Identification of Organic Compounds*, edited by D. Sawicki & J. Stiefel, pp. 91–164. New York: John Wiley & Sons.
- Spek, A. L. (1990). *Acta Cryst.* **A46**, C34.
- Stenhouse, P. J., Valles, E. M., Kantor, S. W. & MacKnight, W. J. (1989). *Macromolecules*, **22**, 1467–1473.
- Sun, H., Mumby, J. S., Maple, J. R. & Hagler, A. T. (1994). *J. Am. Chem. Soc.* **116**, 2978–2987.
- Tanaka, M. & Nakaya, T. (1989). *Makromol. Chem.* **190**, 3067–3088.
- Visser, J. W. (1969). *J. Appl. Cryst.* **2**, 89–95.
- Zlokazov, V. B. & Chernyshev, V. V. (1992). *J. Appl. Cryst.* **25**, 447–451.